Size-Dependent Molecular Dissociation on Mass-Selected, Supported Metal Clusters

U. Heiz,* F. Vanolli, A. Sanchez, and W.-D. Schneider

Contribution from the Institut de Physique Expérimentale, Université de Lausanne, CH-1015 Lausanne, Switzerland

Received April 8, 1998

Abstract: Particles of nanometer size (nanoparticles) supported on well-characterized oxide surfaces are of particular interest to model the high complexity of real catalysts to answer questions such as the role of intrinsic size effects and the influence of the support.[1,2] Model systems so far consisted of size-distributed nanoparticles deposited on oxide substrates,[3−5] which do not allow an unambiguous determination of the cluster's chemical nature. Here, we report on the size-dependent chemical reactivity of nickel clusters, size selected and deposited with low energy (0.2 eV/atom) on thin MgO(100) films. Monodispersed Ni_{30} clusters show a higher reactivity for CO dissociation than Ni_{11} and Ni_{20}. In particular, Ni_{30} clusters are extremely reactive and dissociate up to 10 CO molecules at temperatures below 280 K. Our results demonstrate that such small, supported clusters are unique for catalytic reactions not only due to their high surface-to-volume ratio but essentially because of the distinctive properties of different cluster sizes.

1. Introduction

Industrial catalysts are often made of metal particles (1−10 nm) supported on ill-defined oxide powders. Because of a high surface-to-volume ratio and the coexistence of different facets these particles may show enhanced efficiencies and selectivities for chemical reactions compared to plane surfaces.[6−8] We aim to go beyond this size range and investigate clusters consisting of a few or a few tens of atoms only, as for these sizes the clusters show strongly size-dependent chemical and physical properties.[9−11] Some illustrations of a size effect in the chemical reactivity of free and supported metal clusters have been shown in the past. Kaldor et al. reported chemical reactivities for free clusters of various metals.[12] By mass spectrometry they observed a strong size-dependent behavior of the chemisorption of molecules on small metal clusters. Recent experiments on the chemical reactivity of free metal clusters reported by the groups of Hackett, Riley, and Ervin revealed size-dependent absolute rate coefficients of the reaction of Nb_n clusters with D_2 and N_2[13] and equilibrium constants for the chemisorption reactions of molecular nitrogen with nickel clusters[14] and described catalytic cycles for the oxidation of CO to CO_2 by gas-phase platinum cluster anions.[15] However, these experiments[12−14] can neither give structural details on the adsorption of the molecule to the cluster nor determine whether the molecule is dissociated by a certain cluster size. Fayet et al.[16] and later Leisner et al.[17] showed that the latent-image generation in the photographic process requires silver clusters of a critical size. Development occurred after the specimen was exposed to cluster beams containing Ag_4^+ clusters or larger aggregates. Recently, Xu et al. observed a size-dependent catalytic activity of supported metal clusters for the hydrogenation of toluene by using organometallic precursors.[18] These precursors were decarbonylated to give the size-selected clusters Ir_4 and Ir_6. Unfortunately this method is restricted only to a few metals and sizes, where stable organometallic precursors exist.

Motivated by the lack of methodical investigations of size effects for supported catalysts we demonstrate the possibility to systematically observe simple chemical reactions on size-selected and soft-landed clusters regardless of size and material. We investigated the chemical reactivity of monodispersed nickel clusters, which were deposited with almost thermal energy on thin MgO(100) films, typical substrates for industrial catalysts. In particular, we were able to observe a size dependence of the

(1) Boudart, M.; Djega-Mariadassou, G. *Kinetics of Heterogeneous Catalytic Reactions*; Princeton University Press: Princeton, NJ, 1984.
(2) Gates, B. C.; Guzci, L.; Knoetzinger, H. *Metal Clusters in Catalysis, Studies in Surface Science and Catalysis*; Gates, B. C., Guzci, L., Knoetzinger, H., Eds.; Elsevier: Amsterdam, 1986; Vol. 29.
(3) Andersson, S.; Frank, M.; Sandell, A.; Giertz, A.; Brena, B.; Bruehwiler, P. A.; Martensson, N.; Libuda, J.; Bauemer, M.; Freund, H.-J. *J. Chem. Phys.* **1998**, *108*, 2967−2974.
(4) Frank, M.; Andersson, S.; Libuda, J.; Stempel, S.; Sandell, A.; Brena, B.; Giertz, A.; Bruehwiler, P. A.; Baeumer, M.; Martensson, N.; Freund, H.-J. *Chem. Phys. Lett.* **1997**, *279*, 92−99.
(5) Lambert, R. M.; Pacchioni *Chemisorption and Reactivity on Supported Clusters and Thin Films*; Lambert, R. M., Pacchioni, Eds.; Kluwer Academic Publishers: Dordrecht, 1997; Vol. 331.
(6) Goodman, D. W. *Chem. Rev.* **1995**, *95*, 523.
(7) Hoffmann, F. M.; Dwyer, D. J. *Surface Science of Catalysis: In Situ Probes and Reaction Kinetics*; Hoffmann, F. M., Dwyer, D. J., Eds.; ACS Sym. Ser. No. 482; American Chemical Society: Washington, DC, 1992.
(8) Matolin, V.; Mâsek, K.; Elyakhloufi, M. H.; Gillet, E. *J. Catal.* **1993**, *143*, 492.
(9) Kaldor, A.; Cox, D.; Zakin, M. R. *Adv. Chem. Phys.* **1988**, *70*, 211.
(10) Billas, I. M. L.; Chatelain, A.; deHeer, W. A. *Science* **1994**, *265*, 1682.
(11) Heiz, U.; Vayloyan, A.; Schumacher, E.; Yeretzian, C.; Stener, M.; Gisdakis, P.; Roesch, N. *J. Chem. Phys.* **1996**, *105*, 5574−5585.
(12) Whetten, R. L.; Cox, D. M.; Trevor, D. J.; Kaldor, A. *Phys. Rev. Lett.* **1985**, *54*, 1494.
(13) Berces, A.; Hackett, P. A.; Lian, L.; Mitchell, S. A.; Rayner, D. M. *J. Chem. Phys.* **1998**, *108*, 5476−5490.
(14) Parks, E. K.; Nieman, G. C.; Kerns, K. P.; Riley, S. J. *J. Chem. Phys.* **1998**, *108*, 3731−3739.
(15) Shi, Y.; Ervin, K. M. *J. Chem. Phys.* **1998**, *108*, 1757−1760.
(16) Fayet, P.; Granzer, F.; Hegenbart, G.; Moisar, E.; Pischel, B.; Woeste, L. *Phys. Rev. Lett.* **1985**, *55*, 3002.
(17) Leisner, T.; Rosche, C.; Wolf, S.; Granzer, F.; Woeste, L. *Surf. Rev. Lett.* **1996**, *3*, 1105−1108.
(18) Xu, Z.; Xiao, F.-S.; Purnell, S. K.; Alexeev, O.; Kawi, S.; Deutsch, S. E.; Gates, B. C. *Nature* **1994**, *372*, 346−348.

S0002-7863(98)01181-0 CCC: $15.00
Published on Web 09/05/1998

elementary steps (adsorption, dissociation, and recombination) of the reaction of CO with monodispersed nickel clusters. In contrast to large nickel particles, in the investigated size range almost all atoms constitute the clusters' surface. Going from Ni_{11} to Ni_{30} the average coordination number of the atoms in the cluster as well as the electronic structure is changed, leading to the observed different chemical behavior.

2. Experimental Section

The chosen substrates are thin MgO(100) films, epitaxially grown on a Mo(100) single crystal. These films exhibit properties very similar to those of bulk magnesia.[19] Recent density functional calculations revealed that Ni_4 binds preferentially to the surface oxygen of MgO-(100) by a polar covalent bond, with bond energies of more than 0.5 eV per nickel atom.[20] Pacchioni et al. concluded that the metal−metal bond prevails over the metal−oxygen bond with the consequence that deposited nickel clusters keep their cluster identity. Thus MgO is a well-suited support for size-selected nickel clusters.

The clusters are produced with a recently developed, high-frequency laser evaporation cluster source.[21] In this setup a laser is focused on a metal target. A helium pulse thermalizes the produced metal plasma and the clusters are grown by nucleation when the helium−metal vapor undergoes supersonic expansion. Subsequently the positively charged cluster ions are mass selected by quadrupole mass spectroscopy. The advantage of this cluster source is 2-fold. On the one hand, the generated cluster currents are sufficiently high for depositions under UHV conditions. On the other hand, these clusters have narrow kinetic energy distributions (0.2−2 eV). This allows for deposition of nickel clusters with an energy of less than 0.2 eV per atom, which is a factor of 10−20 smaller than calculated bond energies of bare nickel clusters.[22] Therefore the size-selected clusters are deposited on the substrate with soft impact, which is crucial to prevent fragmentation.[23,24] Upon deposition the cluster ions are neutralized either on defect sites (V^--centers) or by charge tunneling through the thin MgO films. In addition cluster coverages and deposition temperatures are kept low ($T = 90$ K) to prevent coalescence of the clusters. Coverages used in this study are always 1.0×10^{14} nickel atoms per cm^2, e.g., 4.0‰ of a monolayer (ML) Ni_{11}, 2.2 ‰ ML Ni_{20}, and 1.4 ‰ ML Ni_{30}. The monodispersed Ni clusters are then exposed with a molecular beam doser to carbon monoxide. The interaction of CO with the nickel aggregates is studied with Thermal Desorption Spectroscopy (TDS) and Fourier Transform Infrared (FTIR) spectroscopy.

3. Results

The CO desorption spectrum from a clean MgO support (Figure 1A) exhibits one low-temperature peak at about 100 K, assigned to desorption of physisorbed CO.[25] By contrast, the desorption spectrum of CO from Ni_{11} (9.1×10^{12} clusters per cm^2) displays two additional peaks at 240 (M) and 570 K (A) (Figure 1B), attributed to desorption of molecularly adsorbed CO and associatively desorbed CO, respectively (see below). The presence of the low-temperature desorption (100 K) indicates desorption from MgO and shows that the clusters are saturated with CO.[26] The desorption spectrum of CO adsorbed on Ni_{30} (3.3×10^{12} clusters per cm^2) is displayed in Figure 1C

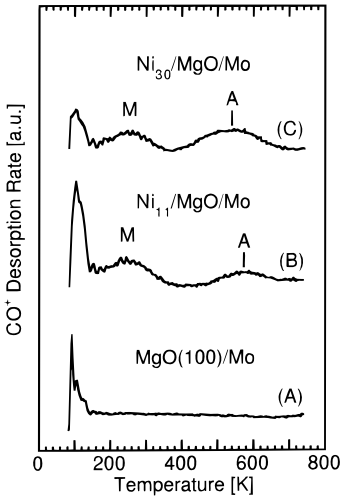

Figure 1. Thermal desorption spectra of carbon monoxide for (A) a MgO(100) film, (B) 9.1×10^{12} Ni_{11} clusters per cm^2, and (C) 3.3×10^{12} Ni_{30} clusters per cm^2. The clusters are deposited at 90 K. The heating rate is 2 deg K/s. Desorption peaks are denoted M for molecular desorption and A for associative desorption. Both cluster coverages represent the same amount of nickel atoms on the surface, i.e., 1.0×10^{14} atoms of nickel per cm^2. From the area of the desorption peaks the number of CO molecules adsorbed on each cluster is calculated (see text).

Table 1. Summary of the Results of the TPD Experiments for Monodispersed Ni_{11}, Ni_{20}, and Ni_{30}[a]

cluster	no. of molecularly bound CO	no. of dissociated CO	dissociated CO per amount of Ni (%)	temp of CO recombination (K)
Ni_{11}	4 ± 0.8	1 ± 0.2	9 ± 1.8	570 ± 20
Ni_{20}	8 ± 1.6	1 ± 0.2	5 ± 1.0	600 ± 20
Ni_{30}	6 ± 1.2	10 ± 2.0	33 ± 6.7	540 ± 20

[a] Shown are the numbers of molecularly and dissociated CO molecules per cluster, the relative amount of reactive Ni atoms for CO dissociation (reactivity), and the temperature of maximal rate of associative desorption (Peak A in Figure 1).

and reveals two desorption peaks at 260 (M) and 540 K (A). Note that the integral of desorption peak A for Ni_{30} is significantly larger than it is for Ni_{11}. The average numbers of desorbing CO molecules from each site of the individual clusters are obtained by integrating the thermal desorption peaks M and A in parts B and C of Figure 1 and normalizing the integral to the amount of clusters on the surface. The TDS system was calibrated by measuring the desorption of CO from a CO-saturated Mo(100) surface, the saturation coverage of which is known.[27] The number of clusters on the surface is directly obtained by integrating the cluster current on the sample. Table 1 summarizes the calculated numbers of molecular and dissociated CO as well as the reactivity for CO dissociation expressed by the relative number of reactive nickel atoms in the cluster and the temperatures of maximal rates of associative desorption for Ni_{11}, Ni_{20}, and Ni_{30}. In a second experiment the deposited clusters are exposed at 90 K to a mixture of isotopically labeled $^{13}C^{16}O$ and $^{12}C^{18}O$. The samples are then heated to 750 K while the desorbing species are analyzed by a mass spectrometer. The result of this experiment is shown in Figure 2 for Ni_{30}. The two low-temperature desorption peaks reveal no isotopic mixing and only $^{12}C^{18}O$ and $^{13}C^{16}O$ are detected for these adsorption sites. At high temperature (540 K), $^{13}C^{18}O$ molecules desorb from the cluster in addition to the two initially adsorbed CO

(19) Wu, M. C.; Corneille, J. S.; Estrada, C. A.; He, J.-W.; Goodman, D. W. *Chem. Phys. Lett.* **1991**, *182(5)* , 472.
(20) Pacchioni, G.; Rösch, N. *J. Chem. Phys.* **1996**, *104*, 7329.
(21) Heiz, U.; Vanolli, F.; Trento, L.; Schneider, W.-D. *Rev. Sci. Instrum.* **1997**, *68*, 1986−1994.
(22) Raghavan, K.; Stave, M. S.; DePristo, A. E. *J. Chem. Phys.* **1989**, *91*, 1904.
(23) Cheng, H.-P.; Landman, U. *J. Phys. Chem.* **1994**, *98*, 3527.
(24) Bromann, K.; Felix, C.; Brune, H.; Harbich, W.; Monot, R.; Buttet, J.; Kern, K. *Science* **1996**, *274*, 956−958.
(25) He, J.-W.; Cesar, A. E.; Corneille, J. S.; Wu, M.-C.; Goodman, D. W. *Surf. Sci.* **1992**, *261*, 167−170.
(26) On a magnesium oxide surface the activation energy for CO migration is lower than the desorption energy, therefore the CO can be trapped by the cluster before it desorbs.
(27) Zaera, F.; Kollin, E.; Gland, J. L. *Chem. Phys. Lett.* **1985**, *121(4/5)*, 464.

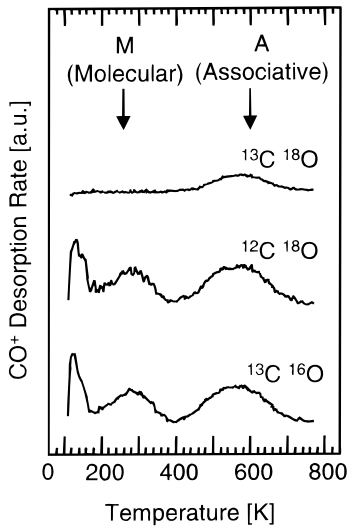

Figure 2. Thermal desorption spectra of an isotopic mixture of $^{13}C^{16}O$ and $^{12}C^{18}O$ adsorbed on Ni_{30} /MgO/Mo. Shown is the desorption of the three isotopes $^{13}C^{16}O$, $^{12}C^{18}O$, and $^{13}C^{18}O$. $^{13}C^{18}O$ can only be formed if carbon monoxide is dissociated by the cluster and subsequently is desorbed associatively. This experiment characterizes different binding sites on the cluster, showing that the low-temperature peaks at around 100 and 260 K originate from molecularly adsorbed CO and the high-temperature peak from dissociated CO. $^{12}C^{16}O$ which is also formed is not shown due to bad signal-to-noise ratio.

species. Panels A and B of Figure 3 display infrared spectra of CO adsorbed on Ni_{11} and Ni_{30} clusters for various annealing temperatures. CO adsorbed on Ni_{11} at 90 K reveals three types of absorption bands at 2081, 1915, and 1398/1324 cm^{-1}. The three bands disappear at temperatures near 330 K. CO adsorbed on Ni_{30} at 90 K exhibits a different behavior (Figure 3B), revealing only two absorption bands at 2084 and 1385/1329 cm^{-1}. The absorption band around 2100 cm^{-1} disappears above 280 K, whereas the untypical low-frequency band at around 1400 cm^{-1} disappears at temperatures below 280 K. Note that the observed intensities of the absorption bands of CO adsorbed on Ni_{30} are different compared to the corresponding ones of CO adsorbed on Ni_{11}.

4. Discussion

To study the size-dependent reactivity of Ni clusters in detail and to directly show that part of the adsorbed CO dissociates on individual clusters TDS is used. Adsorbing a mixture of isotopically labeled $^{13}C^{16}O$ and $^{12}C^{18}O$ (1:1) and analyzing the desorbing species one can directly conclude if the CO molecules on a specific site are adsorbed molecularly or dissociatively. Desorption of the original mixture points to molecular adsorption. Desorption of $^{12}C^{16}O$ and $^{13}C^{18}O$ in addition to the original mixture proves that the cluster dissociates carbon monoxide on the corresponding adsorption site. For Ni_{30} the two low-temperature desorption peaks at 100 and 240 K (Figure 2) reveal no isotopic mixing, and are therefore attributed to binding sites, on which CO is adsorbed molecularly (M). At high temperature (540 K) $^{13}C^{18}O$ is detected, which is produced on the cluster. This isotopic exchange is only possible when CO is first dissociated on the corresponding site of the clusters and then desorbed associatively (A). The dissociation of CO is also inferred from the absence of CO infrared bands above 280 K (Figure 3B). This experiment directly reveals the existence of two differently reactive sites on the nickel clusters. A measure of the different reactivity of the monodispersed Ni_n clusters is the number of adsorbed and dissociated CO on the different binding sites of

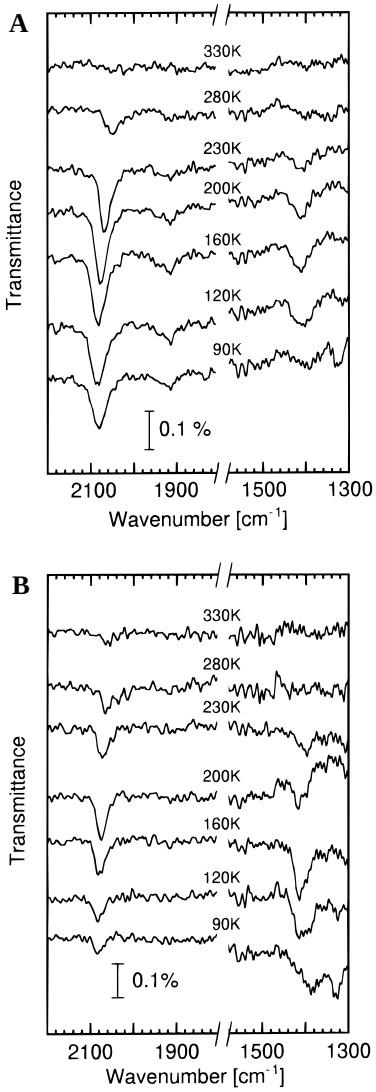

Figure 3. Transmittance infrared spectra of CO adsorbed on Ni_{11} (A) and Ni_{30} (B). CO is adsorbed at 90 K, and the spectra are taken after annealing the sample to the indicated temperatures. Two regions of the IR absorption spectrum are shown, between 1300 and 1600 cm^{-1}, where precursor states for CO dissociation are observed, and between 1800 and 2200 cm^{-1}, the frequency range typical for molecularly bound CO.

each cluster (Table 1). From the spectrum shown in Figure 1B (peak M) we calculate 4 molecularly adsorbed CO molecules per Ni_{11} cluster. The second peak (A) in Figure 1B corresponds to the associative desorption of CO as shown above. Here heating the support to higher temperature leads to recombination of carbon and oxygen, which starts at 400 K and peaks at 570 K. The calculation of the number of dissociated CO on Ni_{11}, based on peak A in Figure 1B, yields 1 ± 0.2, leading to a total of 5 ± 1 CO molecules adsorbed on each Ni_{11} cluster (4 ± 0.8 molecular, 1 ± 0.2 dissociated; see Table 1). It is interesting to note that in the gas-phase Ni_{11} accommodates at most 19 CO ligands, which is about a factor of 4 larger than for the supported cluster.[28] This significant decrease is not surprising as the interaction of the cluster with the support diminishes the number of available adsorption sites. However, in contrast to the present investigation, gas-phase studies cannot disentangle between molecularly and dissociatively bound CO. Ni_{20} adsorbs a total number of 8 ± 1.6 CO molecules, where

(28) Fayet, P.; McGlinchey, M. J.; Woste, L. H. *J. Am. Chem. Soc.* **1987**, *109*, 1733−8.

only 1 ± 0.2 is dissociated (spectrum not shown). Interestingly, Ni_{30} displays a distinctly different behavior. From the spectrum in Figure 1C, a total number of 16 ± 3.2 adsorbed CO's on Ni_{30} is obtained. Here 6 ± 1.2 CO's are molecularly bound and desorb at 260 K and a total of 10 ± 2 molecules are dissociated by the cluster and desorb associatively at 540 K. These results clearly show the size-dependent chemical reactivity of the three nickel cluster sizes.

The characterization of the adsorbed CO on each cluster site and an estimation of the temperature where CO is completely dissociated can be inferred from the results of the infrared studies. In accordance with previous studies of larger, size-distributed nickel particles on silica[29] the bands around 2100 cm^{-1} (Figure 3A/B) may be attributed to terminal CO adsorbed on one nickel atom of the cluster. The band around 1900 cm^{-1} is assigned to CO species bridging two Ni atoms in Ni_{11}. However, infrared spectroscopy alone is insufficient to make such structural assignments. The disappearance of the IR absorption band of terminal CO ($\sim$2100 cm^{-1}; Figure 3A/B) correlates with Peak M in Figure 1A/B. This supports molecular desorption from these sites. In addition, the desorption temperature is close to the value of molecularly adsorbed CO on Ni(100).[30] Such a low temperature implies a weak CO interaction with the clusters. From stepped Ni(111) surfaces and small size-distributed nickel particles (1.6−5.4 nm in size) on mica molecularly bound CO desorbs at higher temperatures between 380 and 430 K.[31] The low-frequency bands (Figure 3A/B) are divided into two parts. It has an unusually low frequency and is similar to the vibrational feature observed at 1520 cm^{-1} on a stepped Ni(111) surface,[32] assigned to CO in a predissociated state. The presence of this band indicates that some of the carbon monoxide is close to being dissociated upon adsorption. The group of Yates, Jr. observed a similar band at around 1500 cm^{-1} originating from CO chemisorbed on small nickel particles deposited on Al_2O_3 with EELS spectroscopy. They relate this CO stretching mode to $Ni_x-C-O-Ni_y$ type species. In addition they found a retardation of the formation of bridged CO, which is directly associated with the formation of this low-frequency $Ni_x-C-O-Ni_y$ species.[33] This is in agreement with the present cluster deposition measurements, since for Ni_{30}, where this band is most pronounced, no bridged CO is observed. For Ni_{11} the low-frequency band at around 1400 cm^{-1} of the precursor state for dissociation disappears between 280 and 330 K (Figure 3A), marking the completion of the decomposition of carbon monoxide. For Ni_{30} this low-frequency band disappears at slightly lower temperatures and therefore decomposition of CO is completed below 280 K (Figure 3B). These IR results show that the decomposition of CO depends not only on the temperature but also on cluster size. The low decomposition temperature of CO on the clusters differs from CO dissociation on polycrystalline films and sputter damaged Ni(111) surfaces, where decomposition is completed at around 400 and 450 K, respectively.[34]

The results presented here convincingly show that *differently sized* supported metal clusters behave chemically different. This may have profound influences in catalysis, especially as these clusters differ in many ways from other nickel materials. One reason for this variation is the high surface-to-volume ratio; in fact in these clusters almost all atoms are exposed to the surface. But such structural arguments are hardly sufficient to explain alone the particular reactivities among the clusters. Much more substantial is the individual electronic character of each cluster and its distinct interaction with the substrate when varying the cluster size. When a CO molecule is approaching a supported cluster there is a subtle interplay between the repulsive electronic interaction in the entrance channel and the availability of appropriate d-electrons of the cluster for an attractive interaction with CO, leading eventually to a partial charge transfer to the antibonding $2\pi^*$ state of the CO molecule.[35] Since these clusters are so small, the size-dependent interaction with the substrate is significant and determines their oxidation state and the polarization of their electronic states.[20] These effects together are decisive for the interaction strength of the CO molecules with the cluster, which may finally lead to the observed size-dependent dissociation of the adsorbed molecule.

Interestingly, we observed an associative desorption at relatively low temperatures for all three size-selected supported nickel clusters. Associative desorption is only observed for stepped Ni(111) surfaces at a temperature of 823 K when heating the sample with high heating rates.[36] For small nanometer-sized particles CO can only be desorbed by oxygen treatment at 520 K.[31] In both cases it was argued that either carbon or oxygen is diffusing into the bulk which then prevents the formation of CO. In small clusters this is not possible, as the bulk simply does not exist. Therefore carbon and oxygen are effectively present on the surface of the clusters after decomposition and desorb associatively at temperatures up to about 600 K, depending on cluster size. This may be important in catalysis, as the carbon and oxygen are present on the clusters and available for further reactions like, e.g., the hydrogenation of carbon or the formation of carbon dioxide.

5. Conclusions

To summarize, we have shown that by varying the cluster size from Ni_{11} to Ni_{30} the average number of dissociated CO on each active site can be changed deliberately. Using these activated atoms for further reactions may result in a high selectivity of a catalyzed reaction at relatively low temperature. These size effects are dominated by the individual character of each cluster composed of a fixed number of atoms, but also, as the comparison with free clusters indicates, the size-dependent interaction with the substrate plays a significant role in changing the bonding properties of such small supported metal clusters. Thus the use of size-selected, supported clusters on thin oxide films is particularly promising for the investigation of size dependencies of simple chemical reactions on small particles, which is an important issue in heterogeneous catalysis.

Acknowledgment. We thank K. Morgenstern and J. Barth for a critical reading of the manuscript. This work has been supported by the Swiss National Science Foundation.

JA981181W

(29) Coulter, K.; Xu, X.; Goodman, D. W. *J. Phys. Chem.* **1994**, *98*, 1245−1249.

(30) Lauterbach, J.; Wittmann, M.; Küppers, J. *Surf. Sci.* **1992**, *279*, 287−296.

(31) Doering, D. L.; Dickinson, J. T.; Poppa, H. *J. Catal.* **1982**, *73*, 91−103.

(32) Erley, W.; Ibach, H.; Lehwald, S.; Wagner, H. *Surf. Sci.* **1979**, *83*, 585−598.

(33) Chen, J. G.; Crowell, J. E.; Yates, J., J. T. *Surf. Sci.* **1987**, *187*, 243−264.

(34) A comparison of the decomposition temperatures with literature values from other nickel species is inaccurate since this is the only study where CO adsorbed on nickel is identified by infrared and thermal desorption spectroscopy. In our results the temperature range of the completion of CO dissociation is 50 K while usually one finds ranges of about 100 to 150 K.

(35) Blyholder, G. *J. Phys. Chem.* **1964**, *68*, 2773.

(36) Erley, W.; Wagner, H. *Surf. Sci.* **1978**, *4*, 333−341.